Renewable and Sustainable Energy Reviews 134 (2020) 110327

Contents lists available at ScienceDirect

Renewable and Sustainable Energy Reviews

journal homepage: http://www.elsevier.com/locate/rser

Advances in multifunctional balanced ventilation technology for dwellings and arising challenge to quantify energy efficiency and renewable generation contributions using international test standards

David Hunt [a,*], Naoise Mac Suibhne [a], Laurentiu Dimache [a], David McHugh [b], John Lohan [a]

[a] Integrated Sustainable Energy Technologies Research Group, Galway-Mayo Institute of Technology, Galway, Ireland
[b] ProAir Heat Recovery Ventilation Systems Ltd., Tuam Road, Galway, Ireland

ARTICLE INFO

Keywords:
Multifunctional balanced ventilation
Heat recovery
Heat pump
Thermal performance
Energy efficiency
Renewable generation

ABSTRACT

This paper evaluates the ability of EN16573:2017 to isolate and quantify the energy efficiency and renewable generation contributions of multifunctional balanced ventilation systems. These systems integrate an air-source heat pump with heat recovery ventilation and two similar, yet physically different configurations (C1 and C2) are assessed. Heat pump operation does not influence heat recovery performance for widely used configuration C1 but does influence for novel configuration C2. This study shows that while EN16573:2017 can isolate the energy efficiency (heat recovery exchanger) and renewable generation (heat pump) contributions for configuration C1, it fails when applied to configuration C2. Measurements undertaken using EN16573:2017 on configuration C2 revealed an overall coefficient of performance of 5.07, split 51% heat exchanger with heat pump off (phase 1), and 49% heat pump (phase 2 minus phase 1). If this result were obtained for configuration C1 the respective contributions would be 51% energy efficiency and 49% renewable generation. While these contributions cannot be resolved using EN16573:2017 for configuration C2, it can be achieved using two additional measurement planes in the incoming airstream. These showed an 88%:12% contribution from the heat exchanger and heat pump, respectively. While accurate, this result under-estimates the true heat pump contribution, as its positive impact on the heat exchanger efficiency boosts its contribution from 51% (phase 1) to 88% (phase 2). This paper acknowledges that heat pump operation leverages a 37% increase in heat exchanger performance and proposes a that the respective contributions of the heat exchanger and heat pump should be 42%:58%.

1. Introduction

The European Union (EU) defines its commitment to a clean energy transition by agreeing binding climate and energy policy targets with each member state. EU wide greenhouse gas emission reduction targets have increased from 20%, relative to 1990, by 2020 [1], to 40% by 2030 [2] and most likely to 100% by 2050, under the emerging European Green Deal [3]. These climate targets are being achieved by a range of measures, including increasing both energy efficiency [4] and the share of renewable energy generation. Indeed, each member state must be able to quantify the extent by which its energy efficiency [5] and renewable generation [6] has increased each year as this data must be reported to the EU. Every energy related project must be capable of quantifying its contribution to improving either energy efficiency, renewable generation, or both. Hence, this paper focuses on means of isolating and quantifying the energy efficiency (EE) and renewable generation (RG) contributions of an emerging green technology.

Since 40% of Europe's final energy consumption is used to meet heating and cooling demands within buildings, the EU has refined its Energy Performance of Building Directives (EPBD) in 2010 and 2018 [7]. The original EPBD (2002) sought improved building energy efficiency in the EU, introducing building integrated renewable generation and building energy ratings. Individual member states have introduced metrics to monitor their compliance and associated primary energy reduction. For example, Ireland introduced two metrics to track improvements in both building energy performance, using the Maximum Permitted Energy Performance Coefficient (MPEPC), and associated carbon emissions using the Maximum Permitted Carbon Performance Coefficient (MPCPC) [8].

These metrics from individual dwellings are then aggregated at national level so that each member state can meet both its EE and RG

* Corresponding author.
E-mail address: david.hunt@research.gmit.ie (D. Hunt).

https://doi.org/10.1016/j.rser.2020.110327
Received 18 December 2019; Received in revised form 28 August 2020; Accepted 29 August 2020
Available online 12 September 2020

Nomenclature

List of symbols

P	capacity or power input, in kW
Q	thermal energy, in kWh
W	electrical work, in kWh
t	time duration, in s
h	specific enthalpy in kJ/kg
q_m	mass flow rate, in kg/s
q_v	volume flow rate, in m^3/s
T	temperature, ^oC

List of subscripts/superscripts

AC	supply Air Cooling
AH	supply Air Heating
WH	(Domestic) hot water production
el	electric
HR	heat recovery
V	ventilation
phase 1	test phase 1
phase 2	test phase 2

List of acronyms/abbreviations

ODA	Outdoor air
SUP	Supply air
ETA	Extract air
EHA	Exhaust air
COP	Coefficient of performance
HRV	Heat recovery ventilation
HP	Heat pump
EE	Energy Efficiency
EHA-HP	Exhaust air source heat pump
ODA-HP	Outdoor air source heat pump
RG	Renewable generation
MFBV	Multifunctional Balanced Ventilation

targets and reporting obligations. However, this is not always straight forward as the integration of EE with RG technologies challenge both the standards organisations and the building energy rating software designers to develop appropriate methods to measure and present the EE and RG contributions of a technology, so that this data can subsequently be translated into a building energy rating. The former issue is investigated in this paper for one such novel integrated technology.

Europe's residential building sector accounts for over 27% of its energy demand, 17% for heating alone [9]. Technological innovations that address this huge market has inspired the integration of heat recovery ventilation (HRV) and heat pumps (HPs). Traditionally, these technologies developed independently to serve the complementary, yet different needs for improved energy efficiency, delivered by HRV, and renewable heating delivered by HPs. However, the integration of both technologies has yielded Multifunctional Balanced Ventilation (MFBV) [10], also referred to as mechanical ventilation heat pump recovery [11], compact heat pumps [12], or thermodynamic heat recovery units [13]. These highly functional integrated systems deliver improved energy efficiency and renewable generation, as well as practical advantages associated with compactness, ease of installation, commissioning, and service. However, as new physical configurations or airflow layouts of these integrated systems emerge, so does the challenge to define, isolate and measure their respective EE and RG contributions. This specific issue has stimulated the current research.

Nguyen et al. [14] developed an experimental heat pump, heat recovery system, that could accommodate four physically different airflow configurations. The experimental analysis identified the combined heat pump and heat recovery ventilation unit as the most energy efficient configuration. Fucci et al. [15] experimentally tested one MFBV unit and reported very high overall system coefficients of performance (COP) that ranged between 6.62 and 9.50. Siegele et al. [16] also experimentally characterised a MFBV unit, with an overall system performance of over 4.5. The wide range of reported overall system COPs not only reflects variation in system design, components, and airflow configurations, but also inconsistency in COP definition and measurement methods. These observations reflected the absence of a universal standard measurement method, consistent with any emerging technology. Also note how most studies use an overall system COP to represent the combined performance of the integrated heat recovery and heat pump components.

The development of test standard EN16573:2017 [11] brought clarity to the measurement methods and definition of key performance metrics. It employed a two-step or two-phase test method, consisting of phase 1 which yields the heat recovery capacity (HRV with HP off), and phase 2 which delivers the overall air heating capacity (HRV with HP on). While the overall heating capacity enables the combined contributions of the heat exchanger and the heat pump to be quantified (phase 2), it does not enable the individual contributions of either component to be resolved simultaneously during phase 2. Instead the HP contribution is established by subtracting the phase 1 result (with HP off) from the phase 2 result (with HP on). Such an approach assumes that heat pump operation does not impact on heat exchanger recovery capacity, so its contribution to the overall air heating capacity remains stable during both phase 1 and phase 2. Indeed, this assumption holds for all the reported system configurations [14–16] and EN16573:2017 delivers all three essential metrics; overall heating capacity, heat recovery capacity (energy efficiency) and heat pump COP (renewable generation). However, EN16573:2017 is unable to deliver the heat pump COP for unit configurations where heat pump operation impacts on heat recovery capacity during phase 2. Possible solutions to this issue are presented in this paper.

Two similar, yet physically different integrated heat pump and heat exchanger configurations are considered in this study. The conventional unit configuration where heat pump operation does not impact on heat exchanger performance is selected from the literature [15]. This configuration is used to highlight the novel unit configuration being experimentally investigated in this work. The construction, operating principles and functionality of both system configurations are contrasted for space heating mode. The standard test methodology is applied to the novel configuration and its ability to characterise the thermal contribution of both the heat exchanger and the heat pump during test phase 2 is assessed. This investigation identified slight modifications to the current standard that would enable it to accommodate a greater diversity of MFBV configurations and deliver a more comprehensive thermal characterisation. Such data not only allows the heat recovery capacity (EE) and heat pump capacity (RG) of MFBV systems to be defined, but also deliver the necessary inputs for the mandatory building performance metrics (MPEPC, MPCPC, BER and RER).

2. International test standards

The five key thermal performance standards are presented in this section and mapped against the characterisation procedure and the functionality of the system being characterised. Test standard implementation is also introduced.

2.1. Matching standards with MFBV configurations

European Standard EN16573:2017 specifies the laboratory test

methods, conditions and requirements for testing the aerodynamic, acoustic and thermal performance of MFBV units intended for use in a single dwelling [10]. The scope includes unit constructions containing one or more of the following features within the casing; (1) supply and exhaust air fans, (2) air filters, (3) common control system, and one or more of the additional components (4) air-to-air heat exchanger, (5) air-to-air heat pump (6) air-to-water heat pump. Table 1 presents six recognised combinations of multifunctional units and their corresponding features (1-to-6). Features 1-to-4 are common to all unit combinations, while the type of heat pump used is either air-to-air and/or air-to-water. All units, as defined by the standards, must contain all features within a single housing.

Note: while other combinations of multifunctional unit are available these do not include an air-to-air heat exchanger and are not covered in this study.

According to EN16573:2017, multifunctional ventilation units shall be designed and controlled to provide a hygienic balanced ventilation rate for occupants in dwellings. Consequently, for unit configurations A-to-F (Table 1), the aerodynamic performance characteristics are tested before or in conjunction with thermal characterisation testing. Aerodynamic characteristics include both internal and external leakage as well as air flow capacity/pressure curves.

Fig. 1 maps the international test standards against the unit configuration and test sequence of unit configurations A-to-D (Table 1). As configurations E and F represent functions that are considered subsets of configuration B, C and D they are not included on Fig. 1 to reduce complexity. EN13141-7:2010 [17] and EN13141-4:2011 [18] are used to identify air leakage and flow/pressure characteristics respectively. Common to all configurations, Fig. 1 highlights the combination of standards EN16573:2017 and EN13141-7:2010, used to identify the starting conditions and initial ventilation measurements.

Test phase 1 conditions are achieved with heat recovery ventilation mode operating and the heat pump switched off. Individually, thermal testing hydronic space heating/cooling and supply air heating/cooling functions are covered by EN14511:2018 (all parts) [19]. Meanwhile, EN16147:2017 [20] covers domestic hot water production. However, as Fig. 1 presents, thermal performance testing of air-to-air heat recovery ventilation and air-to-air heat pumps and/or air-to-water heat pumps are undertaken in accordance with multiple combinations of standards.

2.2. Implementing standards test procedure

This section describes how the relevant standards were implemented for multifunctional unit Configuration C, Table 1, providing heat recovery ventilation and supply air heating. Once the aerodynamic characteristics are established, Fig. 2 illustrates the subsequent two-phase test method. Air flow test conditions, installation and measurements are performed according to EN14511:2018, EN13141-7:2010 and EN16573:2017 (see Fig. 1). As shown in Fig. 4 and Fig. 6, all air condition measurement sensors (dry bulb temperature, relative humidity, volume flow rate) are located in the outdoor air (ODA), supply air (SUP), extract air (ETA) and exhaust air (EHA) duct connections to/from the unit.

Table 1
System functionality and features of six combinations of combined heat pump and heat recovery ventilation multifunctional units defined in EN16573:2017. Features numbered in the table are listed and described in the main text.

Configuration	Combined heat pump and heat recovery ventilation multifunctional units	Features
A[a]	HRV combined with domestic hot water production	1, 2, 3, 4, 6
B[a]	HRV combined with hydronic space heating/cooling	1, 2, 3, 4, 6
C[a b]	HRV combined with supply air heating/cooling	1, 2, 3, 4, 5
D[a]	HRV combined with heating and hot water production	1, 2, 3, 4, 5, 6
E	HRV combined with cooling and hot water production	1, 2, 3, 4, 5, 6
F	HRV combined with hydronic and supply air heating/cooling	1, 2, 3, 4, 5, 6

[a] Sequence of test standards used for aerodynamic and thermal performance characterisation mapped in this study (Fig. 1).

[b] Two different configurations of air-to-air heat exchanger and air-to-air heat pump are characterised in this study.

Measurements used to calculate thermal and electrical performances are identified per test phase. Test phase 1 starts with heat recovery ventilation mode (HP off). During phase 1 the ventilation electrical power input ($P_{el,V}$) is measured, air condition measurements are used to calculate the ventilation heat recovery capacity (P_{HR}). Test phase 2 starts with the heat pump on for either heating or cooling function while simultaneously providing heat recovery ventilation. Operating in space heating mode, measurements taken during test phase 2 are used to calculate the overall supply air heating capacity (P_{AH}), overall heating thermal energy (Q_{AH}) and electrical energy input ($W_{el,V\text{-}AH}$).

Unit configuration C's overall coefficient of performance ($COP_{V\text{-}AH}$), established while simultaneously providing heat recovery ventilation and supply air heating, is calculated using Eq. (1). The overall heating thermal energy (Q_{AH}) is calculated using Eq. (2). P_{AH} is calculated as the ODA mass flow rate ($q_{m,ODA}$) times the incoming airstream, ODA to SUP, specific enthalpy increase (h_{ODA} to h_{SUP}) using Eq. (3). EN16573:2017 does not provide or reference additional standard for an equation to calculate the electrical energy input ($W_{el,V\text{-}AH}$). Therefore, $W_{el,V\text{-}AH}$ is assumed to be the combined total electrical energy consumption of both heat recovery ventilation and heat pump and may be calculated using Eq. (4), based on Eq. (8) given by the standard. A definition of $COP_{V\text{-}AH}$ is not given by the standard, however from Eq. (1), it can be described as the ratio of the supply air heating thermal energy to the electrical energy input. $COP_{V\text{-}AH}$ does not allow the HRV and HP respective energy efficiency and renewable generation contributions to be isolated or measured. Instead these individual component contributions are lumped to give the overall system performance.

$$COP_{V-AH} = \frac{Q_{AH}}{W_{el,V-AH}} \tag{1}$$

$$Q_{AH} = \frac{\int_0^{t_{AH}} P_{AH}\,dt}{3600} \tag{2}$$

$$P_{AH} = q_{m,ODA}\cdot(h_{SUP} - h_{ODA}) \tag{3}$$

$$W_{el,V-AH} = \frac{P_{el,V-AH}\cdot t_{AH}}{3600} \tag{4}$$

Supply air heating coefficient of performance (COP_{AH}) is calculated using Eq. (5). The thermal energy recovered ($Q_{HR\text{-}AH}$) by the heat exchanger is calculated using Eq. (6). Heat recovery capacity (P_{HR}) is calculated using Eq. (7), based on measurements recorded during test phase 1. The electrical energy input ($W_{el,V}$) is calculated using Eq. (8), based on measured electrical power input ($P_{el,V}$) during test phase 1. While a definition of COP_{AH} is not given, it can be described based on Eq. (5) as the ratio of the increased supply air thermal energy ($Q_{phase,2\ (HP+HRV)}$ minus $Q_{phase,1\ (HRV)}$) to the increased electrical energy consumed by the heat pump in phase 2 ($W_{el,phase,2\ (HP\ ON)}$ minus $W_{el,phase,1\ (HP\ OFF)}$).

$$COP_{AH} = \frac{Q_{AH} - Q_{HR-AH}}{W_{el,V-AH} - W_{el,V}} \tag{5}$$

$$Q_{HR-AH} = \frac{P_{HR}\cdot t_{AH}}{3600} \tag{6}$$

$$P_{HR} = q_{m,SUP}\cdot(h_{SUP} - h_{ODA}) \tag{7}$$

$$W_{el,V} = \frac{P_{el,V}\cdot t_{AH}}{3600} \tag{8}$$

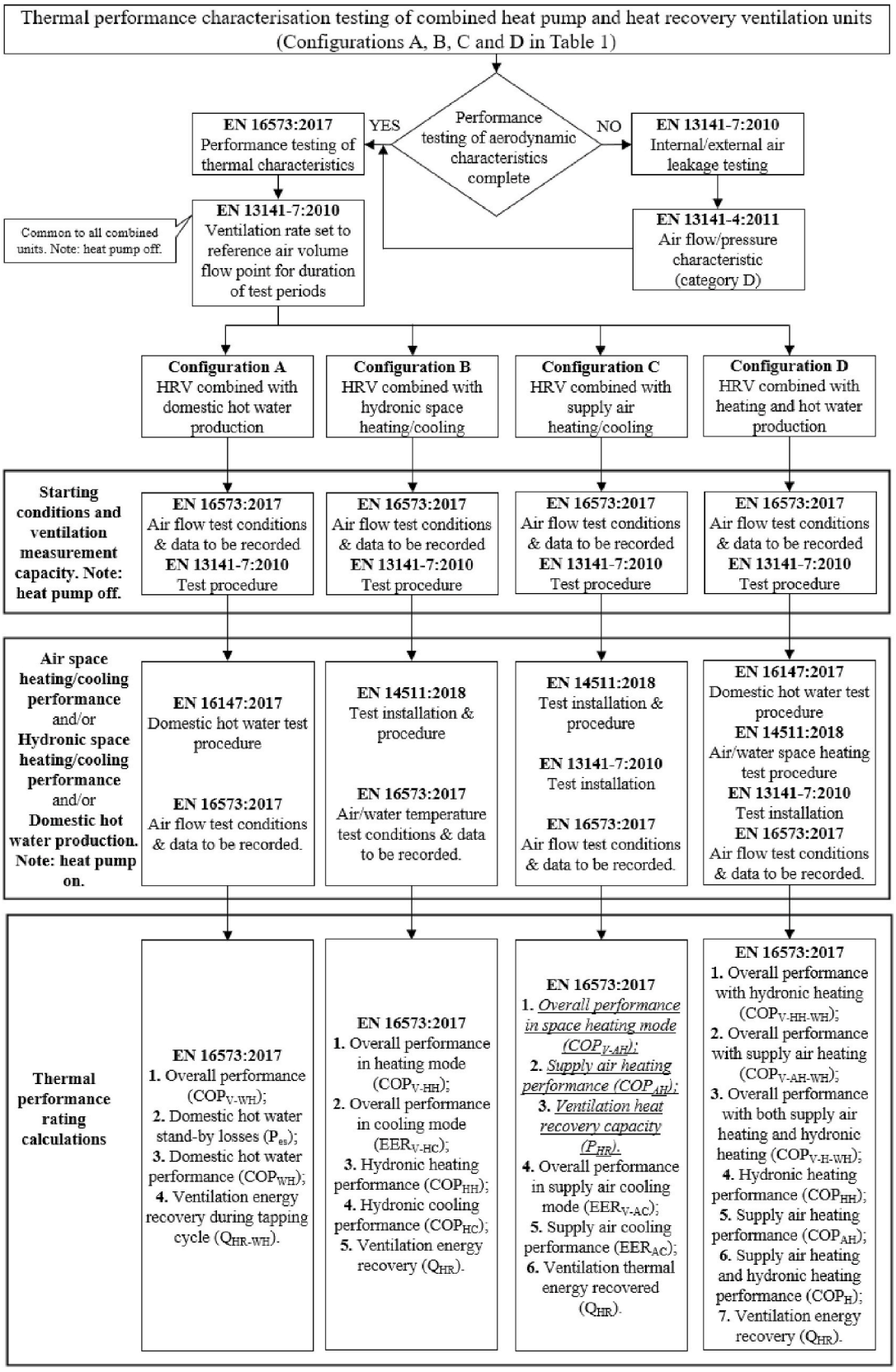

Fig. 1. Mapping the relevant international test standards required to conduct aerodynamic and thermal performance characterisation of unit configuration A to D (Table 1). Note, aerodynamic testing, starting conditions and ventilation measurement are common to all unit configuration A-to-F presented in Table 1. Text *underlined* identifies the performance metrics that are subject to discussion in this paper.

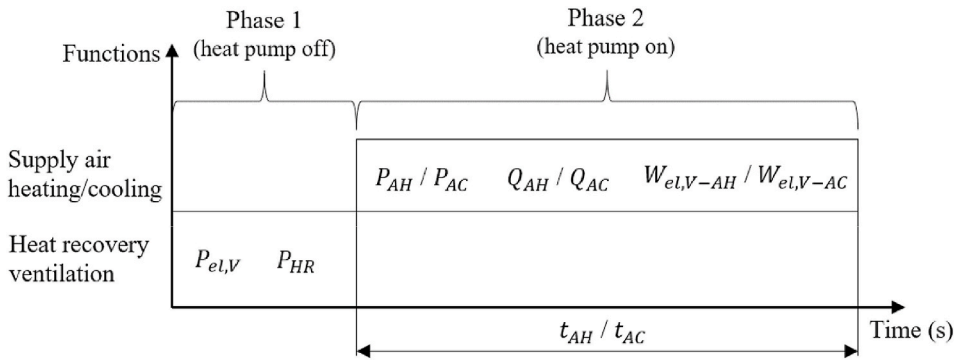

Fig. 2. Two-phase thermal performance test procedure for heat recovery ventilation combined with supply air heating/cooling (Configuration C, Table 1).

EN16573:2017 provides additional specifications while referring to EN13141-7:2010, EN14511:2018 and EN16147:2017. Combined, the standards give a comprehensive description of the test setup, conditions, procedures, and equations. However, while many possible unit configurations and wide-ranging functionalities are considered, the novel outdoor-air heat pump (ODA-HP), with both direct expansion coils located either side of the heat exchanger in the incoming airstream is not referenced in any standard. As a result, this paper assesses the ability of EN16573:2017 to isolate and measure the ventilation heat recovery capacity (EE) and heat pump capacity (RG) for this novel configuration.

3. Configuration C - multifunctional ventilation unit layout

The default function of domestic MFBV systems are to extract stale air (ETA) from inside the building while simultaneously supplying fresh air (SUP) to the building. The SUP and ETA ventilation rates are balanced, ensuring that equal volumes of air enter and leave the building [21]. A balanced mechanical ventilation system provides a pressure distribution that has an approximate neutral impact on the building [22]. For the purpose of thermal performance testing, a unit is declared balanced if the SUP and ETA mass flow rates are within 3% of each other (EN13141-7:2010) or unbalanced if they deviate by more than 10% (EN16573:2017).

Heat recovery ventilation systems are the single most important means of reducing ventilation energy consumption [23] and can provide significant energy savings for mechanically ventilated residential buildings [24]. Guillén-Lambea et al. analysed the space heating and cooling energy demand requirements of nearly zero-energy buildings (nZEB) and concluded that these limits cannot be achieved with current ventilation strategies in cold climates, without heat recovery [25]. In general, heat recovery ventilation can be classified as either sensible or enthalpy recovery [11,26]. Sensible heat recovery increases the incoming airstream's temperature, without any change to its humidity. Enthalpy (sensible and latent heat) recovery increase both the temperature and humidity of the incoming airstream. In terms of total thermal energy recovered, sensible recovery devices generally have lower efficiency than enthalpy recovery devices [27,28]. Both devices are passive recovery systems, as no additional energy is needed to recover heat [15]. A review of heat recovery ventilation devices and air-to-air heat and mass exchanger technologies for building applications are available in Refs. [29,30] respectively.

Typically, heat pump classification is based on the identification of the thermal source and sink [31]. A configuration C unit may utilise a reversable refrigerant flow, air-to-air source heat pump that employs air as both the thermal source and sink. The two configurations of unit C investigated in this paper are referred to as unit C1 and C2 and their configurations are presented in Figs. 4 and 6 respectively.

Operating in HRV mode, Fig. 3 illustrates the variation in the incoming and outgoing airstream conditions (temperature and humidity ratio) through configuration C during test phase 1 (HP off). In an ideal system, the heat transferred from the warm outgoing air is equal to the heat recovered by the cooler incoming air. This is presented as increasing/decreasing temperature gradients across the heat exchanger. However, during experimental testing an error band exists between heat transferred/recovered and may vary by up to ±15% [21] and ±20% [32]. This is mainly due to a combination of internal/external air leakage and unaccounted heat transfer between the unit and the surrounding air. Measurements recorded at ODA, SUP, ETA and EHA duct connections are used to calculate the heat recovery capacity ($P_{HR,phase\ 1}$) for both configurations C1 and C2 using Eq. (6). In addition, sensible and latent efficiencies on both the supply and exhaust air sides can be calculated according to EN13141-7:2010. Both configurations operating in space heating mode are discussed in detail in the following sections.

3.1. C1 configuration - exhaust air heat pump with sensible heat exchanger

The conventional C1 configuration shown in Fig. 4 combines an exhaust air heat pump (EHA-HP) with a sensible heat exchanger [14,15] operated in space heating mode. The incoming fresh airstream (labelled 1-to-6) is conditioned by a serial, 2-stage, passive and active heat recovery process. ODA (1) enters the heat exchanger core (3), where sensible energy is passively recovered before entering the HP condenser coil (4). The HP condenser coil actively increases the SUP sensible energy before entering the building (6). The location of the HP evaporator coil (9) utilises the heat exchanger core outgoing EHA as the heat source. Subsequently, unit configuration C1 provides four functions; ventilation, heat recovery ventilation (no moisture recovered), space heating and space cooling.

Fig. 5 illustrates the corresponding changes in the incoming and outgoing airstream's temperature and humidity ratio during space heating mode (HP on). The heat removed from the EHA by the evaporator coil comprises of sensible heat plus latent heat of condensation [33]. These processes are presented in Fig. 5 by the EHA dry bulb temperature and humidity ratio, respectively. The EHA dry bulb temperature and humidity ratio both decrease as the HP evaporator coil absorbs its heat. When the cooling EHA reaches saturation temperature, moisture condenses on the evaporator coil [34] triggering the potential to also recover latent heat of condensation [35]. On the SUP side, the HP condenser coil adds sensible heat. The dry bulb SUP temperature increases due to the positive temperature difference between the SUP air and the condenser coil.

Fucci et al. [15] described the MFBV configuration in Fig. 4 as "passive plus active recovery system". Similar to EN16573:2017, Fucci et al. defined an overall system coefficient of performance (COP_s) as the ratio of the heat output of the system to the electric power consumed by the system. However, two key factors differentiate COP_s from the overall performance proposed in EN16573:2017 and defined by Eqs. (1)–(4). Firstly, COP_s utilises the SUP mass flow rate to calculate the heat output, whereas Eq. (3) utilises the ODA mass flow rate; and secondly, only the

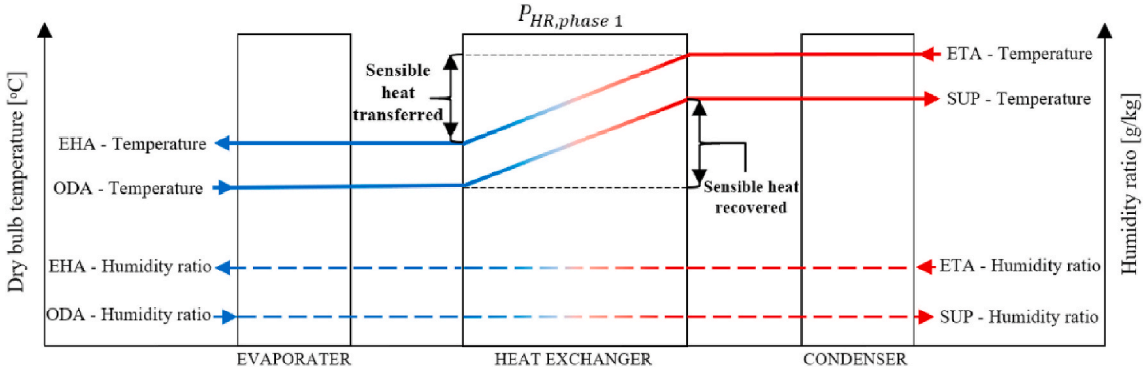

Fig. 3. Test phase 1, illustration of incoming and outgoing air conditions (dry bulb temperature and humidity ratio) for both configurations during heat recovery ventilation mode.

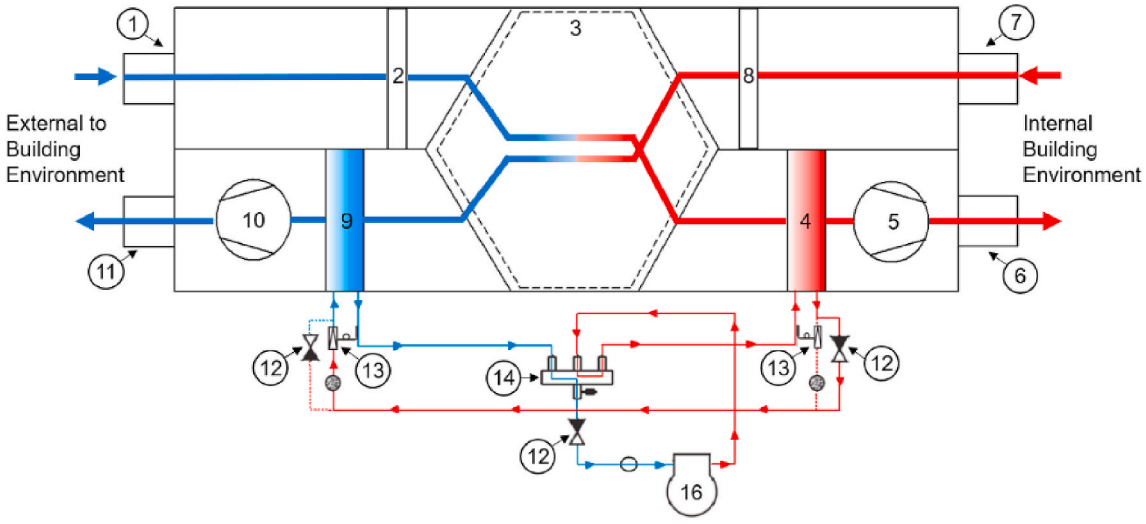

Fig. 4. Unit configuration C1 operating in space heating mode: (1) outdoor air - ODA; (2) supply air filter; (3) air-to-air heat exchanger core; (4) HP, condenser coil; (5) supply air fan; (6) supply air - SUP; (7) extract air - ETA; (8) extract air filter; (9) HP, evaporator coil; (10) extract air fan; (11) exhaust air - EHA; (12) NRV - non return valve; (13) TEV - thermostatic expansion valve; (14) 4-way valve; (16) compressor.

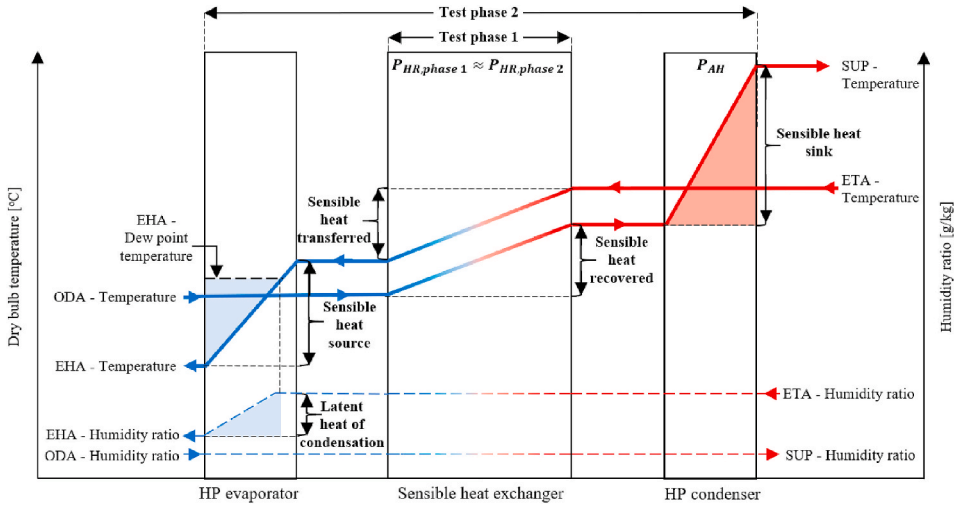

Fig. 5. Charting the notional variation in air flow dry bulb temperature and humidity ratio for configuration C1 operating in space heating mode; during test phase 2 (HP on).

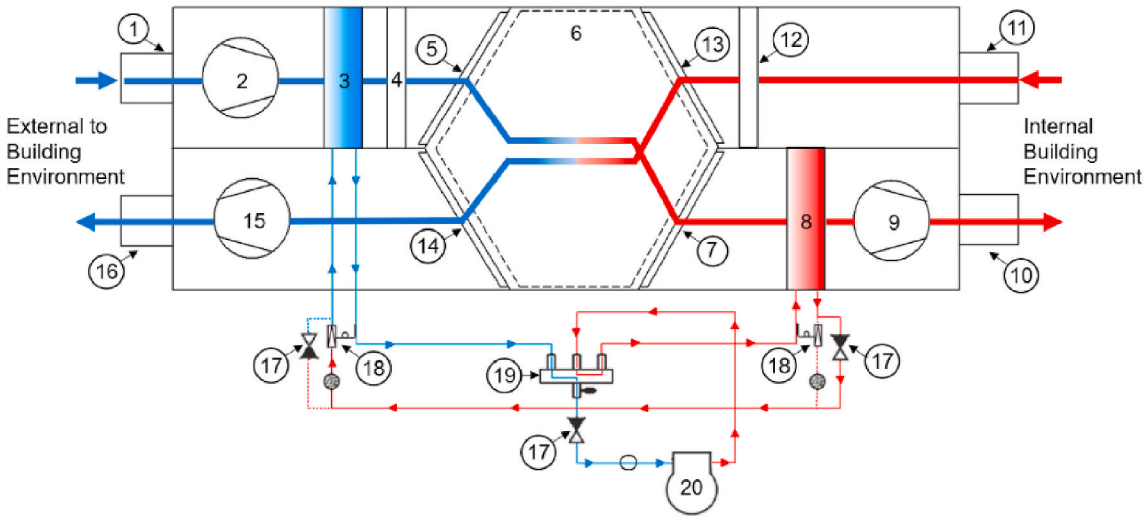

Fig. 6. Unit configuration C2 operating in space heating mode: (1) outdoor air - ODA; (2) secondary supply air fan; (3) HP, evaporator coil; (4) supply air filter; (5) ERV, motorised slider 1; (6) air-to-air enthalpy exchanger core; (7) ERV, motorised slider 4; (8) HP, condenser coil; (9) primary supply air fan; (10) supply air - SUP; (11) extract air - ETA; (12) extract air filter; (13) ERV, motorised slider 3; (14) ERV, motorised slider 2; (15) extract air fan; (16) exhaust air - EHA; (17) NRV - non return valve; (18) TEV - thermostatic expansion valve; (19) 4-way valve; (20) compressor.

sensible heat output is quantified when calculating COP_s, whereas Eq. (3) considers both sensible and latent heat. Hence, COP_s is not equivalent to $COP_{V\text{-}AH}$. This highlights the subtle differences that exist between system performance factors defined in the literature and the standard, making it difficult to compare results.

Nguyen et al. [14], also studied sensible heat recovery during heating and ventilation and described the integrated configuration in Fig. 4 as "double heat recovery". Similarly, yet not identical to EN16573:2017, this study considered two kinds of COP: net coefficient of performance (COP_{net}) and refrigerant based coefficient of performance (COP_{ref}). COP_{net} is described as the ratio of air-based net heating capacity to the electric power consumption of the compressor. However, COP_{net} is not comparable with Eqs. (1)–(4) as the overall air-based net heating capacity is calculated using the SUP mass flow rate, whereas Eq. (3) utilises the ODA mass flow rate. Equally, only the compressor electrical consumption is considered. Hence, COP_{net} is not equivalent to $COP_{V\text{-}AH}$. Meanwhile, COP_{ref} represents the ratio of the HP condenser heating capacity to the electric power consumption of the compressor. Consequently, COP_{ref} is also not comparable with the air heating performance Eq. (5) ($COP_{ref} \neq COP_{AH}$). The HP condenser air heating capacity is calculated using the SUP mass flow rate and the specific enthalpy across the HP condenser coil.

Siegele et al. [16] experimentally analysed a MFBV unit. This study proposed two kinds of COP: overall system coefficient of performance (COP_{sys}) and heat pump coefficient of performance ($COP_{HP,sys}$). COP_{sys} is defined as the ratio of the sum of the systems air heating capacities (supply air condenser, recirculation air condenser and heat recovery ventilation) to the sum of electrical power (compressor, inverter, ambient air fan, recirculation air fan and ventilation air fans). Again, this COP_{sys} equation is not identical to Eq. (1) ($COP_{sys} \neq COP_{V\text{-}AH}$) as the air heating capacity is based on the sum of the individual heating contributions. $COP_{HP,sys}$ is described as the ratio of the sum of the HP air heating capacity (supply air condenser and recirculation air condenser) to the sum of electrical power consumed by the compressor, inverter, ambient air fan and recirculation air fan. Equally, $COP_{HP,sys}$ is not comparable with the air heating performance Eq. (5) ($COP_{HP,sys} \neq COP_{AH}$).

From section 2.2, the overall coefficient of performance from EN16573:2017 ($COP_{V\text{-}AH}$, Eq. (1)), is described as the ratio of the supply air thermal energy to the electrical energy input. The overall supply air heating capacity (P_{AH}, Eq. (3)), based on unit configuration C1 principle of operation, is the sum of the HP condenser and heat exchanger heating capacities. Therefore, $COP_{V\text{-}AH}$ for configuration C1 can be described as the ratio of the sum of the HP's condenser thermal energy delivered and heat exchanger thermal energy recovered to the electrical energy consumed by compressor, inverter, controller, and ventilation air fans.

The supply air heating coefficient of performance (COP_{AH}, Eq. (5)), is described as the ratio of the increased supply air heating thermal energy to the increased electrical energy input due to the heat pump operating in test phase 2, but switched off during test phase 1. Based on system configuration C1's principle of operation, the HP condenser thermal energy delivered (Q_{cond}) can be established by subtracting the heat exchanger's thermal energy recovered during test phase 1 ($Q_{HR\text{-}AH}$) from the sum of the HP condenser thermal energy delivered and heat exchanger thermal energy recovered during phase 2. In this way, the EN standard's two-phase test methodology can distinguish the respective contributions of the HP and HRV as well as the sum of both yielding the overall air heating capacity. Therefore, COP_{AH} can also be considered as the heat pump coefficient of performance (COP_{HP}). However, these conclusions only remain valid if the HP does not affect the ventilation heat recovery capacity. This aspect will be addressed by the C2 configuration.

3.2. C2 configuration - outdoor air heat pump with reverse-flow enthalpy exchanger

The novel C2 configuration shown in Fig. 6 combines an outdoor air heat pump (ODA-HP) with a reverse-flow enthalpy exchanger operating in space heating mode. While the HP thermal source for configuration C1 is the outgoing exhaust airstream, the HP draws its heat from the incoming airstream for configuration C2. This is facilitated by moving the HP evaporator from the exhaust duct (item 9 in Fig. 4), to the supply air duct (item 3 in Fig. 6) with both the condenser and evaporator coils now positioned on either side of the enthalpy exchanger. The novel reverse-flow enthalpy exchanger utilise motorised sliders (items 5, 7, 13 and 14 in Fig. 6) to periodically reverse the air flow direction through the enthalpy exchanger core (item 6). The dwell time between each flow reversal is dictated by ambient humidity conditions and as a result the dwell time can be altered to provide a degree of humidity control [36].

The incoming fresh airstream (items 1-to-10 in Fig. 6) is conditioned (temperature and humidity) by a 3-stage process, involving the heat pump evaporator coil, reverse-flow enthalpy exchanger and heat pump

condenser coil, respectively. In stage 1, ODA enters the unit (1) and is cooled (sensible energy) and dehumidified (latent energy) as it passes through the HP evaporator coil (3). In stage 2, the incoming air is warmed and humidified (optional) as it passes through the reverse-flow enthalpy exchanger (6). Sensible and latent heat is transferred from the outgoing to the incoming airstream within the enthalpy exchanger. During stage 3, the heat pump condenser coil (8) further increases the fresh air temperature (sensible energy) before entering the occupied space (10).

The thermal characteristics/performance of this integrated configuration has not been previously described in the literature and cannot be described as double heat recovery or passive plus active heat recovery as defined by Nguyen et al. and Fucci et al. respectively. This is solely due to the changed location of the HP evaporator coil that utilises the incoming ODA as a heat source. This combined with the novel reverse-flow enthalpy exchanger enables configuration C2 to dehumidify (HP evaporator) and humidify (reverse-flow enthalpy exchanger) the incoming airstream. It is important to note that the reverse-flow enthalpy exchanger can operate at an outdoor air temperature of −15 °C without the need for frost protection [37]. Without this functionality, configuration C2 would not work as the condition of air leaving the evaporator coil may cause frost formation within the enthalpy exchanger core.

Clearly there is a need to establish the thermal performance characteristics of the C2 configuration and the next section describes the application of EN16573:2017 for this purpose.

4. Experimental results and discussion

Aspects of both the experimental facility and experimental results obtained for configuration C2 following the EN16573:2017 standard are presented and discussed in this section. The limitations of the standard are identified, and suggestions are made to the experimental procedure and analysis to address these limitations and augment the standard.

4.1. Measurement equipment and accuracy

As illustrated in Fig. 1, the thermal characterisation of configuration C2 was undertaken in accordance with test standards EN13141-7:2010, EN14511:2018 and EN16573:2017. The air volume flow rates for ODA, SUP, ETA and EHA was recorded using four Badger Vortex RWG40 flow meters. The air temperature at each duct connection was recorded with a 5-point measurement plane using PT100 resistance temperature sensors evenly distributed over the duct cross-section. These utilised a 4-wire RTD measurement system with a commercially available load resistor and sensing unit from National Instruments. The air humidity in each duct was recorded using a Vaisala HMP110 humidity sensor, with an Aplisens PRE-50G pressure transducer used on each duct to set-up and record static air pressure.

Table 2 summarises the monitored parameters and corresponding sensor measurement accuracy. The data from each sensor was logged and stored electronically. Temperature readings from 41 temperature probes were logged twice per second. Data from four pressure sensors, four flow meters and power meter were also recorded twice per second.

Table 2
Measured parameters and associated measurement accuracy.

Parameters	Brand	Type	Accuracy
Temperature	OMEGA	Pt100 (4-wire)	±0.15 °C
Relative humidity	VAISALA	HMP110	±1.5% RH
Air volume flow rate	Badger Meter	Vortex RWG40	±1%
Air Pressure	APLISENS	PRE-50G	±0.6%
Electrical Power	YOKOGAWA	WT310E	0.1% reading + 0.05% range

The humidity sensors logged data at a slower rate of one sample every six seconds from each of the six sensors.

4.2. Limitations of EN16573:2017 for configuration C2

Table 3 presents data recorded for system C2 operating in space heating mode (test phase 2, heat pump on). Values in this table are based on averages during test phase 2 data collection period as shown in Fig. 7.

Fig. 7 shows the thermal power calculated at each of the four measurement planes ODA, SUP (incoming airstream), ETA and EHA (outgoing airstream) over the 7-h long test procedure as defined in Fig. 2. The data in Fig. 7 shows the thermal power fluctuations during seven distinct time periods that traverse test phase 1 (HP off) and test phase 2 (HP on). Test phase 1 consists of a 60-min steady state period #1 followed by a 30-min data collection period #2. Steady state conditions ensure that all measured thermodynamic quantities (Table 2) remain constant with respect to the tolerances given in EN13141-7:2010. Test phase 2 consists of 5 distinct time periods. Once the 30-min steady state period #3 has elapsed, the heat pump is switched on. There is then a 10-min preconditioning period #4 and a 5-min forced heat pump defrost cycle #5. Preconditioning ensures that all measured thermodynamic quantities (Table 2) remain constant with respect to the tolerances given in EN14511–3:2018. This is then followed by a 60-min equilibrium period #6 and a 70-min data collection period #7. The cyclic fluctuations of the SUP and EHA thermal power (Fig. 7) during time periods #6 and #7, result from each reversal of the flow direction through the enthalpy exchanger.

It is the data collected during the phase 1 “data collection period #2” that is used to calculate the ventilation heat recovery capacity (P_{HR}). This is equivalent to the energy efficiency (EE). Test phase 2 “data collection period #7” is used to calculate the overall heating capacity ($P_{AH\text{-}V}$). Subtracting phase 1 from phase 2 yields the supply air heating performance (P_{AH}). This allows the HP contribution ($P_{HP\text{-}cond}$) to be defined as the HP operates during phase 2 but switched off during phase 1. This is equivalent to the renewable generation (RG).

Based on the measured data in Table 3, an overall coefficient of performance ($COP_{AH\text{-}V}$, Eq. (1)) of 5.07 is calculated during phase 2 as per the standard. Where, the overall heating thermal energy (Q_{AH}, Eq. (2)), overall heating capacity (P_{AH}, Eq. (3)) and electrical energy input ($W_{el,V\text{-}AH}$, Eq. (4)) are calculated as 1.56 kWh, 1.23 kW and 0.31 kWh, respectively. Following the EN16573:2017 standard, P_{AH} is calculated as the ODA mass flow rate ($q_{m,ODA}$) times the incoming airstream specific enthalpy increase (h_{ODA} to h_{SUP}). However, if P_{AH} is calculated using the SUP mass flow rate ($q_{m,SUP}$) as in the literature [14–16], $COP_{AH\text{-}V}$ falls by 5% to 4.84. While the recorded SUP volume flow rate (152.1 m^3/h) in Table 3 was marginally greater than the ODA volume flow rate (146.0 m^3/h), the 5% performance decrease in the SUP mass flow was due to the ODA and SUP density difference, calculated as 1.26 kg/m^3 and 1.15 kg/m^3 respectively. Q_{AH} and P_{AH} are calculated as 1.49 kWh and 1.17 kW, respectively.

EN16573:2017 revealed an overall coefficient of performance of 5.07 (1225 W), which can be apportioned 51% heat exchanger with heat pump off (phase 1, Figs. 7, 625 W), and 25% heat pump (phase 2, Fig. 7, 600 W), provided heat pump operation does not impact heat exchanger performance. However, Fig. 7 shows that this assumption is not valid for the C2 configuration.

Supply air heating performance (COP_{AH}, Eq. (5)) is defined as the ratio of the increased supply air thermal energy to the increased electrical energy consumed due to the heat pump operating in test phase 2, but switched off during test phase 1. COP_{AH} of 3.40 is calculated as per the standard. Where, during test phase 1, the thermal energy recovered by the heat exchanger ($Q_{HR\text{-}AH}$, Eq. (6)), heat recovery capacity (P_{HR}, Eq. (7)) and electrical energy input ($W_{el,V}$, Eq. (8)) are calculated as 0.80 kWh, 0.62 kW and 0.08 kWh, respectively. However, as HP evaporator and condenser coils are both located in the incoming airstream, theoretically the coefficient of performance cannot exceed 1. Therefore the

Table 3
Thermal performance quantities recorded during system C2 test phase 2 data collection period.

Variables measured	Symbol	Unit	Outgoing air stream		Incoming air stream			
			ETA (11)	EHA (12)	ODA (21)	SUP (22)	Inlet-HR	Outlet-HR
Ambient air temperature of system C2	$T_{ambient}$	°C	20.03					
Dry bulb temperature	T_{db}	°C	19.99	5.79	6.99	32.94	−0.15	19.20
Relative humidity	RH	%	36.60	75.97	86.76	14.59	98.71	32.49
Air volume flow rate	q_v	m^3/h	148.86	150.0	146.03	152.08	–	–
Duct static pressure	DSP	Pa	101.38	2.87	11.15	92.08	–	–
Electrical voltage	–	V	233.87					
Electrical current	–	A	1.64					
Electrical power input	$P_{el,V-AH}$	W	241.52					
Electrical power factor	–	cosØ	0.63					
Measurement period according to EN14511	t_{AH}	s	4589					

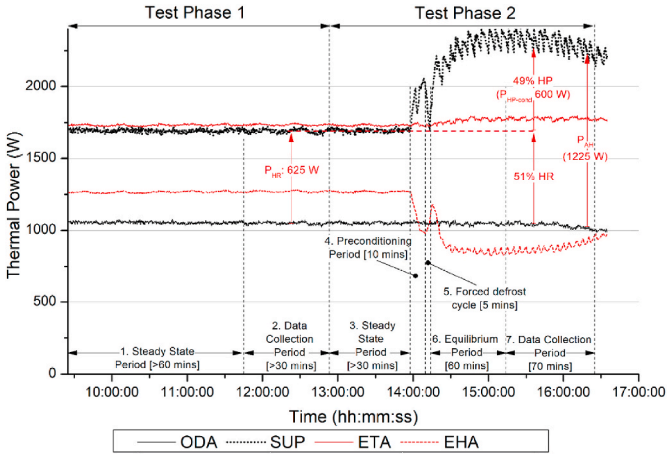

Fig. 7. Incoming (ODA to SUP) and outgoing (ETA to EHA) airstreams thermal power calculated for respective inlet and outlet duct connection measurement planes during test phase 1 and 2 defined in EN16573:2017.

COP_{AH}, of 3.40 is not an accurate reflection of the heat pump contribution.

The increase of the SUP thermal power during time periods #6 and #7 reflect thermal power input from the HP's condenser (item 8 in Fig. 6), as well as an increased thermal contribution from the enthalpy exchanger from phase 1. Activating the HP evaporator (item 3 in Fig. 6) absorbs heat from the incoming air (ODA), thereby cooling the ODA before entering the enthalpy exchanger. This increases the temperature difference between the counter-flowing airstreams within the enthalpy exchanger, which can boost the heat recovery capacity [33–36]. Fernandez-Seara et al. [21] conducted an experimental analysis of an air-to-air heat exchanger. Results identified that the heat transfer rate between the outgoing to the incoming airstreams increased from 300 W, to 525 W, to 700 W as the incoming outdoor air temperature decreased from 15 °C, to 10 °C, to 5 °C respectively. When compared with data collection period #2, the decrease EHA thermal power during data collection period #7 equates to 419 W. This quantifies the additional heat removed from the outgoing airstream during phase 2, thereby highlighted that the HP operation impacts on heat exchanger performance. As a result, the supply air heating capacity (P_{AH}) can no longer be reliably estimated as its calculation (phase 2 minus phase 1) assumes that the enthalpy exchanger recovery capacity remains constant during both phases 1 and 2.

Quantifying the individual contributions of the HRV and HP for the C2 configuration could be achieved by augmenting the EN16573:2017 standard measurement procedure by adding two additional internal measurement planes. These measurement planes are located at the inlet and outlet of the enthalpy exchanger and used to measure temperature and relative humidity of the incoming airstream. A similar technique was also applied to the C1 configuration by previous researchers [14–16]. These two measurement planes were deployed along with the standard ODA, SUP, ETA and EHA measurement planes for configuration C2 and the results are presented in the following section.

4.3. Augmenting EN16573:2017 for configuration C2

Two additional internal temperature measurement planes were setup in the incoming airstream, located at the inlet and outlet of the enthalpy exchanger. These consisted of a 10-point temperature measurement plane with sensors evenly distributed over the enthalpy exchanger's air inlet and outlet sections. In addition, a 2-point humidity measurement plane using Vaisala HMP110 humidity sensors were evenly distributed over the enthalpy exchanger's air inlet section. Table 2 presents sensor measurement accuracy. Fig. 8 shows the thermal power for each of the incoming airstream measurement planes, ODA, SUP, and the two additional measurement planes at the inlet and outlet of the enthalpy exchanger, identified as Inlet-HR, and Outlet-HR, respectively.

The salient features of Fig. 8 are: the marked increase in ventilation heat recovery capacity between phase 1 ($P_{HR,phase\ 1}$) and 2 ($P_{HR,phase\ 2}$); the cyclic fluctuations in data during time periods #6 and #7; and the impact of the HP evaporator cooling capacity ($P_{HP\text{-}evap}$) and HP condenser heating capacity ($P_{HP\text{-}cond}$). In addition to Fig. 7, the cyclic fluctuations of the Outlet-HR thermal power (Fig. 8) during time periods #6 and #7, also result from each reversal of the flow direction through the enthalpy exchanger. The decrease of the Inlet-HR thermal power (Fig. 8) is due to the HP evaporator coil (item 3 in Fig. 6) using the ODA as a thermal source. Activating the HP evaporator absorbs heat from the incoming air (ODA), thereby cooling Inlet-HR as indicated by the lower thermal power data during time periods #6 and #7. This highlights one potential benefit of locating the evaporator in the incoming fresh air

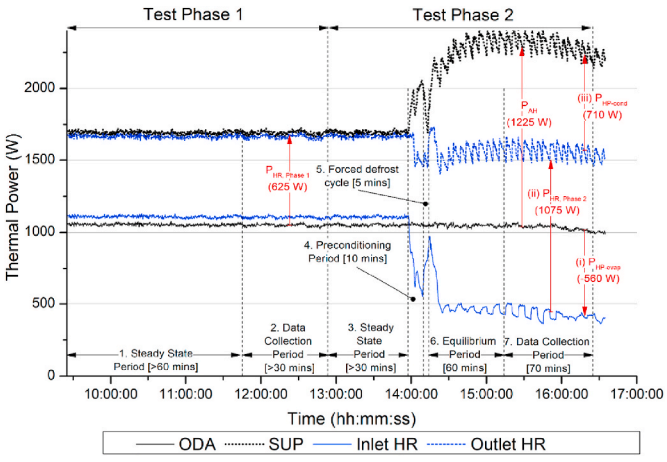

Fig. 8. Incoming airstream thermal power calculated for two mandatory and two additional internal measurement planes during both test phase 1 and 2.

stream. However, this observation also clearly demonstrates that the HP operation impacts heat exchanger performance.

Fig. 9 maps experimental results from configuration C2 of the incoming and outgoing airstream conditions (measured temperature and calculated humidity ratio) during test phase 2. From Table 3, recorded data averaged over data collection period 2 (>70 min) identified that the ODA enters the HP evaporator coil at 6.99 °C and leaves at −0.15 °C, increasing the temperature difference across the enthalpy exchanger (ETA to Inlet-HR) by 7.14 °C. The air flow direction through the enthalpy exchanger is reversed every 300 s, enabling moisture recovery [36,37]. As a result, the incoming air humidity ratio increased by 0.6 g/kg_{dry_air} through the enthalpy exchanger.

Fig. 10 maps experimental results from configuration C2 of the incoming airstream thermal power during both test phase 1 (dotted line, Figs. 10) and 2 (dashed line). As previously discussed, the overall supply air heating capacity (P_{AH}, Eq. (3)) is calculated as per the standard to be 1.23 kW. Alternatively, from Fig. 10, P_{AH} can be calculated as the sum of the HP evaporator cooling capacity ($P_{HP\text{-}evap}$; a negative term) plus the enthalpy exchanger ($P_{HR,phase,2}$) and HP condenser ($P_{HP\text{-}cond}$) heating capacities. The individual contributions, $P_{HP\text{-}evap}$, $P_{HR,phase,2}$ and $P_{HP\text{-}cond}$ are calculated as −560 W, 1075 W and 710 W, using Eq's (10), (11) and (12), respectively. In either case, the application of the direct measurement method (Eq. (3)) or the sum of the individual contributions measurement method (Eq. (9)), yields the same overall coefficient of performance of 5.07.

$$P_{AH} = q_{m,ODA} \cdot (h_{SUP} - h_{ODA}) = P_{HP-evap} + P_{HP-cond} + P_{HR,phase,2} \quad (9)$$

$$P_{HP-evap} = q_{m,ODA} \cdot (h_{\text{inlet-HR}} - h_{\text{ODA}}) \quad (10)$$

$$P_{HR,phase,2} = q_{m,ODA} \cdot (h_{\text{outlet-HR}} - h_{\text{inlet-HR}}) \quad (11)$$

$$P_{HP-cond} = q_{m,ODA} \cdot (h_{\text{SUP}} - h_{\text{outlet-HR}}) \quad (12)$$

From Fig. 10, the increased supply air heating capacity, P_{AH} minus P_{HR}, is calculated as 600 W, due to the heat pump operating in test phase 2, but switched off during test phase 1. Alternatively, the increased supply air heating capacity is equal to the sum of $P_{HP\text{-}evap}$ (−560 W), $P_{HP\text{-}cond}$ (710 W) and the increased heat recovery capacity (450 W). Application of either method, direct measurement (Eq. (3)) or the sum of the individual contributions measurement (Eq. (9)), the supply air heating coefficient of performance is calculated as 3.40. The 42% (450 W) increase in heat recovery capacity is due to the unique location of the HP evaporator coil, increasing the temperature difference across the enthalpy exchanger by 7.14 °C. Based on configuration C2, COP_{AH} reflects the net HP contribution ($P_{HP\text{-}evap}$ and $P_{HP\text{-}cond}$) plus the leveraging effect of the HP evaporator on the enthalpy exchanger.

Traditionally, the heat pump contribution to supply air heating capacity ($P_{HP\text{-}cond}$) and heating thermal energy ($Q_{HP\text{-}cond}$) are calculated using Eq. (12) and Eq. (13), as 710 W and 0.91 kWh, respectively. Accordingly, the heat pump coefficient of performance calculated using Eq. (14) is 4.02. Fig. 11 shows the thermal power for each of the incoming airstream measurement planes, ODA, SUP, and one additional measurement plane at the outlet of the enthalpy exchanger (Outlet-HR). The overall coefficient of performance of 5.07 (1225 W), now split 42% heat exchanger with heat pump off (phase 2, Figs. 11, 515 W), and 58% heat pump (phase 2, Figs. 11, 710 W).

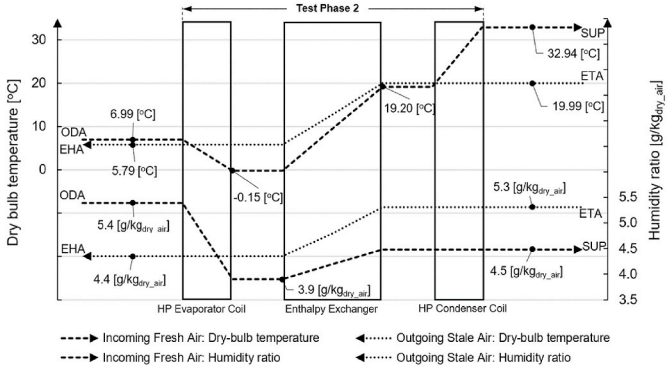

Fig. 9. Recorded data charting the variation in air flow dry bulb temperature and humidity ratio for configuration C2 operating in space heating mode; during test phase 2 at the standards rating operating conditions.

$$Q_{HP-cond} = \frac{P_{HP-cond} \cdot t_{AH}}{3600} \quad (13)$$

$$COP_{HP-AH} = \frac{Q_{HP-cond}}{W_{el,V-AH} - W_{el,V}} \quad (14)$$

However, as the HP evaporator coil is also located in the incoming airstream, the net contribution to supply air heating capacity ($P_{HP\text{-}net}$) and heating thermal energy ($Q_{HP\text{-}net}$) are calculated using Eq. (15) and Eq. (16), as 150 W and 0.19 kWh, respectively. The net heat pump coefficient of performance calculated using Eq. (17) is 0.85.

$$P_{HP-net} = P_{HP-cond} + P_{HP-evap} \quad (15)$$

$$Q_{HP-net} = \frac{P_{HP-net} \cdot t_{AH}}{3600} \quad (16)$$

$$COP_{HP-net} = \frac{Q_{HP-net}}{W_{el,V-AH} - W_{el,V}} \quad (17)$$

Utilising the additional internal measurement planes are essential to quantify the contribution of the integrated technologies and to investigate the standards test methodology when applied to a unique configuration. From Fig. 10, simultaneous measurement of test phase 2, the overall coefficient of performance is calculated as 5.07, $P_{HR,phase,2}$ and $P_{HP\text{-}net}$ are calculated as 1075 W and 150 W using Eqs. (11) and (15), respectively. As a result, the percentage contributions for the enthalpy exchanger is 88% while HP is 12%. Similarly, from Fig. 10, using the standards two-phase test method, the overall coefficient of performance is calculated as 5.07, where P_{AH} is calculated as 1225 W using Eq. (3). However, the supply air heating coefficient of performance is calculated as 3.40, where the increased supply air heating capacity, P_{AH} minus P_{HR}, is calculated as 600 W, due to the heat pump operating in test phase 2, but switched off during test phase 1. In this way, the increased supply air heating capacity due to the HP operation, is equal to the sum of $P_{HP\text{-}net}$ (150 W) and the increased heat recovery capacity (450 W). As a result, the percentage contributions for the enthalpy exchanger (P_{HR}, 625 W) is 51% while HP (600 W) is 49%.

5. Conclusion

The ability of EN16573:2017 standard's two-phase test methodology to identify and quantify the thermal performance characteristics of multifunctional balanced ventilation units has been experimentally investigated. The study focused on two similar, yet physically different configurations (C1 and C2) of a combined air-to-air heat exchanger and air-to-air heat pump operating in space heating mode. While the standard's two-phase test methodology can accurately measure the overall coefficient of performance ($COP_{AH\text{-}V}$ of 5.09) of both configurations it fails to isolate and measure the heat pump (renewable contribution) for the C2 configuration. It has been identified that this failing stems from an underlying assumption that heat pump operation does not impact on heat exchanger performance. While this assumption holds for the C1 configuration, it does not hold for the C2 configuration, as the heat pump evaporator is located downstream of the enthalpy exchanger.

The heat recovery capacity during test phase 1 (625 W) is not equal to the heat recovery capacity during test phase 2 (1075 W, as calculated using the simultaneous measurement method). The unique location of the heat pump evaporator coil increased the temperature difference

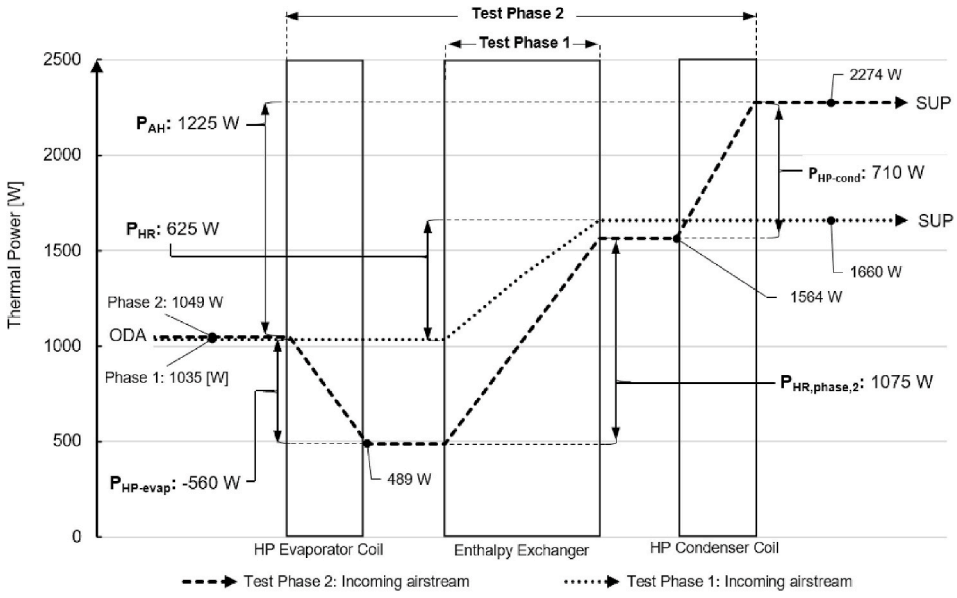

Fig. 10. Comparison of incoming fresh air stream thermal energy recorded during test phase 1 and test phase 2.

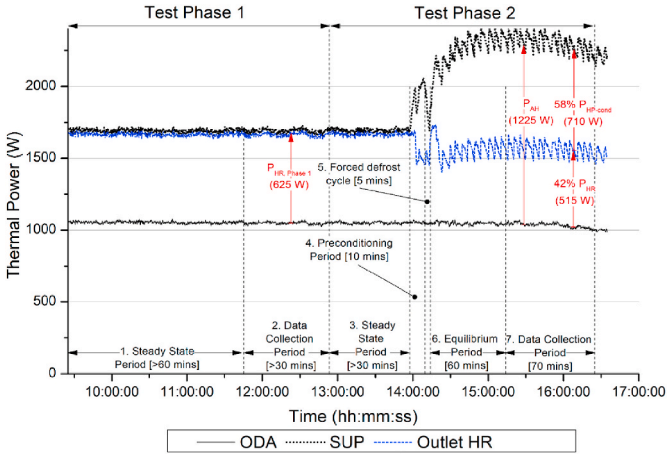

Fig. 11. Incoming airstream thermal power calculated for two mandatory and one additional internal measurement planes during both test phase 1 and 2.

across the enthalpy exchanger by 7.14 °C, this led to a 42% (450 W) increase in the heat recovery capacity. As a result, the supply air heating coefficient of performance is calculated as 3.40. The percentage contributions for the enthalpy exchanger (P_{HR}, 625 W) is 51% while HP (P_{AH}, 600 W) is 49%. These results highlight how the current standard quantify the energy efficiency and renewable generation by measuring primary contributions of both the HP and enthalpy exchanger. However, with the addition of the measurement planes we can further see that the heat pump has separate contributions. In this context, the increased supply air heating capacity due to the HP operation, is equal to the sum of $P_{HP\text{-}net}$ (150 W) plus the increased heat recovery capacity (450 W), where this additional increase may be considered a secondary contribution by the enthalpy exchanger. In such a scenario, the percentage contributions for the enthalpy exchanger increases to 88% (1075 W including both primary and secondary contributions) while HP is 12% (150 W). The additional measurement planes offer a useful insight into the individual and dynamic contributions of the HP and enthalpy exchanger for novel unit configurations, such as the one studied in this work. Efforts to quantify the respective contributions of the heat exchanger and heat pump can be summarised as follows; 51%: 49% (EN16573:2017, Fig. 7); 88%:12% (two additional measurement planes, Fig. 8); and 42%:58% (one additional measurement plane, Fig. 11). Of these options this paper concluded that the 42%:58% heat exchanger heat pump contribution best reflected the operation of this integrated system.

Credit author statement

David Hunt: Conceptualization, Methodology, Investigation, Validation, Formal analysis, Writing - Original Draft, Writing - Review & Editing. **Naoise Mac Suibhne**: Conceptualization, Methodology, Writing - Original Draft, Writing - Review & Editing, Visualization. **Laurentiu Dimache**: Conceptualization, Methodology, Writing - Original Draft, Writing - Review & Editing. **David McHugh**: Resources. **John Lohan**: Conceptualization, Methodology, Supervision, Writing - Original Draft, Writing - Review & Editing.

Declaration of competing interest

The authors declare that they have no known competing financial interests or personal relationships that could have appeared to influence the work reported in this paper.

Acknowledgment

The authors would like to acknowledge the financial support of the European Regional Development Fund (ERDF) under Ireland's European Structural and Investment Funds Programmes 2014–2020; grant agreement IP/2018/0719.

References

[1] European Commission - COM (2006) 545 final. Action plan for energy efficiency: realising the potential. 2006. https://doi.org/10.1017/CBO9781107415324.004.
[2] European Commission - COM (2014) 15 final. A policy framework for climate and energy in the period from 2020 to 2030. 2014. https://doi.org/10.1017/CBO9781107415324.004.
[3] European Commission - COM (2019) 640 final. The European green deal. 2019. https://doi.org/10.1017/CBO9781107415324.004.
[4] Pérez-Lombard L, Ortiz J, Pout C. A review on buildings energy consumption information. Energy Build 2008;40:394–8. https://doi.org/10.1016/j.enbuild.2007.03.007.
[5] European Parliament. Directive (EU) 2018/2002 of the European parliament and of the council of 11 december 2018 amending directive 2012/27/EU on energy efficiency. http://data.europa.eu/eli/dir/2018/2002/oj; 2018.

[6] European Parliament. Directive (EU) 2018/2001 of the European Parliament and of the Council of 11 December 2018 on the promotion of the use of energy from renewable sources. 2018. http://data.europa.eu/eli/dir/2018/2001/oj.
[7] Union European. Energy performance of buildings. Counc. Dir.; 2010. p. 13–35. http://www.buildup.eu/en/practices/publications/directive-201031eu-energy-performance-buildings-recast-19-may-2010.
[8] Minister for the environment heritage and local government. Building Regulations 2011 Technical Guidance Document L Conservation Conservation of Fuel and Energy - Dwellings 2017. http://www.environ.ie/en/DevelopmentHousing/BuildingStandards/.
[9] European Commission. Energy consumption and use by households. 2016. accessed, https://ec.europa.eu/eurostat/web/products-eurostat-news/-/DDN-20180322-1. [Accessed 15 April 2019].
[10] CEN. EN 16573:2017: ventilation for Buildings - performance testing of components for residential buildings - multifunctional balanced ventilation units for single family dwellings. Brussels: including heat pumps; 2017.
[11] Mardiana-Idayu A, Riffat SB. Review on heat recovery technologies for building applications. Renew Sustain Energy Rev 2012;16:1241–55. https://doi.org/10.1016/j.rser.2011.09.026.
[12] Passive House Institute Database, Component Database, (n.d.). https://database.passivehouse.com/en/components/list/compact_heat_pump_unit.
[13] Fabrizio E, Seguro F, Filippi M. Integrated HVAC and DHW production systems for zero energy buildings. Renew Sustain Energy Rev 2014;40:515–41. https://doi.org/10.1016/j.rser.2014.07.193.
[14] Nguyen A, Kim Y, Shin Y. Experimental study of sensible heat recovery of heat pump during heating and ventilation. Int J Refrig 2005;28:242–52. https://doi.org/10.1016/j.ijrefrig.2004.07.022.
[15] Fucci F, Perone C, La Fianza G, Brunetti L, Giametta F, Catalano P. Study of a prototype of an advanced mechanical ventilation system with heat recovery integrated by heat pump. Energy Build 2016;133:111–21. https://doi.org/10.1016/j.enbuild.2016.09.038.
[16] Siegele D, Ochs F, Feist W. Novel speed-controlled exhaust-air to supply-air heat pump combined with a ventilation system. Appl Therm Eng 2019;162:114230. https://doi.org/10.1016/j.applthermaleng.2019.114230.
[17] CEN. EN 13141-7: ventilation for buildings - performance testing of components/products for residential ventilation - Part 7: performance testing of a mechanical supply and exhaust ventilation units (including heat recovery) for mechanical ventilation systems. 2010. Brussels.
[18] CEN. EN 13141-4: ventilation for buildings - performance testing of components/products for residential ventilation - Part 4: fans used in residential ventilation systems. 2011. Brussels.
[19] CEN. EN 14511:2018 Air conditioners, liquid chilling packages and heat pumps for space heating and cooling and process chillers. Brussels: with electrically driven compressors; 2018. Parts 1-4.
[20] CEN. EN 16147:2017 Heat pumps with electrically driven compressors - testing, performance rating and requirements for marking of domestic hot water units. 2017. Brussels.
[21] Fernández-Seara J, Diz R, Uhía FJ, Dopazo A, Ferro JM. Experimental analysis of an air-to-air heat recovery unit for balanced ventilation systems in residential buildings. Energy Convers Manag 2011;52:635–40. https://doi.org/10.1016/j.enconman.2010.07.040.
[22] Chartered institution of building services engineers. CIBSE guide A: environmental design. seventh ed.. 2006. https://doi.org/10.1016/B978-0-240-81224-3.00016-9. London.
[23] Liu D, Zhao FY, Tang GF. Active low-grade energy recovery potential for building energy conservation. Renew Sustain Energy Rev 2010;14:2736–47. https://doi.org/10.1016/j.rser.2010.06.005.
[24] Cuce PM, Riffat S. A comprehensive review of heat recovery systems for building applications. Renew Sustain Energy Rev 2015;47:665–82. https://doi.org/10.1016/j.rser.2015.03.087.
[25] Guillén-Lambea S, Rodríguez-Soria B, Marín JM. Review of European ventilation strategies to meet the cooling and heating demands of nearly zero energy buildings (nZEB)/Passivhaus. Comparison with the USA. Renew Sustain Energy Rev 2016;62:561–74. https://doi.org/10.1016/j.rser.2016.05.021.
[26] hee Choi Y, Song D, Seo D, Kim J. Analysis of the variable heat exchange efficiency of heat recovery ventilators and the associated heating energy demand. Energy Build 2018;172:152–8. https://doi.org/10.1016/j.enbuild.2018.04.066.
[27] Gendebien S, Bertagnolio S, Lemort V. Investigation on a ventilation heat recovery exchanger: modeling and experimental validation in dry and partially wet conditions. Energy Build 2013;62:176–89. https://doi.org/10.1016/j.enbuild.2013.02.025.
[28] Rasouli M, Simonson CJ, Besant RW. Applicability and optimum control strategy of energy recovery ventilators in different climatic conditions. Energy Build 2010;42:1376–85. https://doi.org/10.1016/j.enbuild.2010.03.006.
[29] O'connor D, Calautit JKS, Hughes BR. A review of heat recovery technology for passive ventilation applications. Renew Sustain Energy Rev 2016;54:1481–93. https://doi.org/10.1016/j.rser.2015.10.039.
[30] Zeng C, Liu S, Shukla A. A review on the air-to-air heat and mass exchanger technologies for building applications. Renew Sustain Energy Rev 2017;75:753–74. https://doi.org/10.1016/j.rser.2016.11.052.
[31] ASHRAE, HVAC Systems, Equipment. Applied heat pump and heat recovery systems. 2016 [Chapter 8].
[32] Chen Y, Yang H, Luo Y. Experimental study of plate type air cooler performances under four operating modes. Build Environ 2016;104:296–310. https://doi.org/10.1016/j.buildenv.2016.05.022.
[33] Jones WP. Air conditioning engineering. In: Chapter 3. fifth ed. 2001. https://doi.org/10.1016/B978-075065074-8/50005-0. The psychrometry of air conditioning processes.
[34] ASHRAE. HVAC systems and equipment, mechanical dehumidifiers and related components. 2016 [Chapter 25].
[35] Gustafsson M, Dermentzis G, Myhren JA, Bales C, Ochs F, Holmberg S, Feist W. Energy performance comparison of three innovative HVAC systems for renovation through dynamic simulation. Energy Build 2014;82:512–9. https://doi.org/10.1016/j.enbuild.2014.07.059.
[36] Hunt D, Mac Suibhne N, Dimache L, Mchugh D, Lohan J. Thermal performance characterisation of a reverse-flow energy recovery ventilator for a residential building application. In: E3S web conf.; 2019. p. 3–8. https://doi.org/10.1051/e3sconf/201911101010.
[37] Feist W. Certified passive house component. 2019. https://database.passivehouse.com/en/components/details/ventilation_small/jablotron-living-technology-sro-futura-l-1032vs03.